Радиофизика и радиоастрономия, 1996, т.1, № 1, 94-103

УДК 550.388.2

Near-Caustic Fields and Ionospheric Sounding

V. G. Galushko and Yu. M. Yampolski

Institute of Radio Astronomy National Academy of Sciences of Ukraine 4 Krasnoznamennaya str., 310002 Kharkov, Ukraine

A paper is received by editor June 28, 1995; after remaking January 19, 1996

Results of investigating the spatial and temporal HF field structure near the skip distance are presented. The data were obtained on midlatitude radio paths less than 1000 km in length, using broadcasting stations as sources of the probe signals. The signals reflected by the ionosphere were received and processed with a multichannel coherent receiver and the large phased array of the decameter radio telescope UTR-2. The strong dependence of the probe signal parameters on the ionospheric plasma conditions has allowed formulating and solving a number of model inverse problems of ionospheric diagnostics. It proves possible to determine parameters of the parabolic ionospheric layer, and the effective electron collision frequency, to evaluate horizontal gradients of the electron density and some parameters of the medium scale-size ionospheric irregularities. A number of tests made both within the method and by means of comparison of the restored parameters against the data of other diagnostic techniques demonstrate the high potential and accuracy of the approach described in the paper.

1. Introduction

The main requirements to modern radio systems for remote sounding of the circumterrestrial space are the high spatial and temporal resolution and accuracy of restoration of the medium parameters. To match these conditions, special transmitters of sufficient power, with complicated kind of the signal modulation are used. Meanwhile, in the case of radio propagation through inhomogeneous media, the probe signal may happen to be concentrated in particular spatial areas and show especially high sensitivity to parameters of the propagation channel in such areas. It concerns the near-caustic regions in the vicinity of which even small changes of the propagation conditions lead to significant variations in the signal parameters, which makes these regions very suitable for solving problems of radio diagnostics. It makes possible in some cases to use the already existing sources of radio emission instead of dedicated transmitters. In the paper this possibility is illustrated by the example of ionospheric diagnostics, where the radiation of a broadcasting station has been used as the probing signal.

The wave field behavior near a caustic has been analyzed in many theoretical and experimental papers. The theoretical investigations are in most cases aimed at developing techniques for the calculation of near-caustic fields and analyzing their region of validity (see, for example, Warren, et al., 1982; Kryukovski, et al., 1984; Babitch, et al., 1984; Anyutin and Borovikov, 1984). The experimental works concern, in general, determination of pre-caustic field parameters (like amplitudes, Doppler frequency shifts, periods of fading etc.) for different radio paths and ionospheric conditions (see, for example, Argo, 1993; Taraschuk, et al., 1982; Chernov and Zhyltsov, 1982). But, to the best of the authors' knowledge no attempts made to use the near-caustic fields in ionospheric diagnostics. Below, a review of the several approaches to the appropriate inverse problems is given. The experimental results include the data that have been collected since 1980's.

2. Measurment technique

All the experimental results presented in the paper as an illustrative material, have been obtained by the authors with the use of a special measuring facility set up at the Institute of Radio Astronomy, Ukrainian National Academy of Sciences (Kharkov, Ukraine) in mid-1980's. The measuring complex is located on the territory of the Radio Astronomy Observatory in the vicinity of Kharkov. A characteristic distinction of the complex is the use of the unique phased array of the world largest decameter wavelength radio telescope UTR-2 as the receiving antenna [Braude, et al., 1978]. It has a T-shaped configuration, the largest arm of which (North-South) is 1800 m × 50 m in size and oriented along the meridian. The other sub-array (East-West) is 900 m × 50 m in size and oriented normally to the first one. Both antennas are six row arrays, each of them consists of broad-band dipoles of horizontal polarization. The total number of such elements is 2042. The operating frequency range of the UTR-2 is 7 to 25 MHz . A conversion matrix forms a five-beam

knife reception pattern of the North-South array and a single beam pattern of the East-West antenna. The beamwidth of the resulting pattern is $25'$ at 25 MHz. The electrically steerable beams can be oriented independently for each sub-array. The azimuthal coverage is $\pm 180^{o}$, while the cone in elevation angle is 5^{o} to 90^{o}. Although the UTR-2 is before all a radio telescope, aimed at radio astronomy observations, its long time usage as a HF direction finder has shown the high potential of the antenna in determining angles of arrival for the signals from ground based stations. In particular, this concerns short, single-hop radio paths less than 1000 km in length. For such radio paths it is possible to measure elevation angles with an accuracy $\Delta\varepsilon \cong 1^{o}$. As will be shown below, measurements as precise as this provide separation of the interfering spatial components of the HF signals near the skip distance.

To record the signals reflected by the ionosphere, a special multichannel highly sensitive receiver was used. It is 8-channel coherent superheterodyne receiver with three conversions of the signal frequency. All the three local oscillators are synchronized with the high stability reference oscillator (rubidium generator). As a result, the relative frequency instability of each channel $\Delta f / f_0$ is less than 10^{-9} within the frequency operating range (7 to 25 MHz). After the third frequency conversion, signals at the difference frequency (usually units of Hz) are fed to low frequency filters of three fixed bandwidth, namely 4, 10, and 20 Hz. The use of narrow band filtering makes it possible to separate the radio-frequency carrier of the broadcasting stations that normally have highly stable master oscillators. This way, non-dedicated transmitters can be used for analyzing the Doppler frequency shifts (DFS) of the ionospheric signals to an accuracy about 0,01 Hz. To determine angles of arrival, an amplitude measuring technique is used. The reception patterns of the two sub-arrays are scanned independently to obtain the elevation angle and azimuth dependences of the signal amplitudes. They are stored in a computer permitting quasi real time direction finding. The receiving complex being a multichannel one, various measuring regimes can be effectuated, such as simultaneous recording of signals at different frequencies, use of a set of spaced single dipoles or crossed antennas of a polarimeter. The measured data are stored in a hard disk of a computer with an analog-digital converter and a multichannel tape-recorder. Pre-processing of the data can be conducted with a spectrum analyzer.

Taking into account the midlatitude location of the receiving site and the sizable number of broadcasting stations within a circle 1000 km in radius, it is possible to find for any time a suitable radio line where the operating frequency f_0 would be close to the maximum usable-one (MUF) f_{MUF}. This enables conducting long term observations of the HF field behavior near the caustic surface trace. Since the angular selectivity of the largest arm North-South is the best along the meridian, radio paths of this orientation are preferable for the measurements. The results given below were obtained on the Moscow-Kharkov radio path about 700 km in length.

3. Experimental data

The most complete information on the spatial and temporal distribution of HF fields near the caustic surface trace (CST) could be obtained with the use of a set of spaced receivers located in the vicinity of the skip distance. Taking into account the characteristic scale-size of the HF near-caustic field (NCF) (hundreds of meters to kilometers, depending on the path length and ionospheric conditions) it should require tens of reception points. Evidently, such an experiment is complicated enough to be conducted. There is, however, another, simpler way to obtain the data of interest. Owing the regular (diurnal changes of the electron density profile $N_e(r,t)$) and stochastic (medium- and large-scale fluctuations in the electron density profile caused, for example, by TIDs) variations of the ionospheric parameters, the CST moves permanently along the Earth's surface. If the propagation path length and the operating frequency are fixed, then the CST may cross the reception point. Provided spatial shifts of the caustic are small enough, the hypothesis of uniform motion can suitably describe the variations of the near-caustic HF field distribution. As will be shown below, this approach is quite justified and fruitful when Δx is of order of units of kilometers. Some inadequacy of the approach does not ruin the situation, moreover allows dynamics of the parameter changes to be detailed.

In Fig.1a, a three-channel record of the HF signals is shown. The record was obtained when the CST crossed three spaced single dipoles. The geometry of the dipole location and orientation of the two first interference minima (dash lines) are shown in Fig.1b. Cross-correlation analysis makes it possible to check the hypothesis of uniform

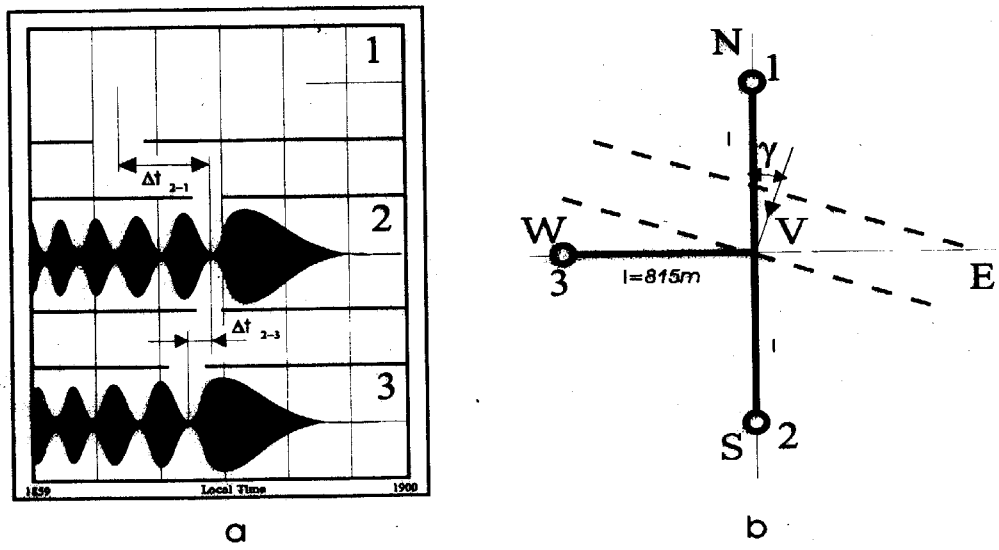

Fig. 1. *A three channel record of the HF signal obtained in the vicinty of the skip distance using three spaced dipoles (a); geometry of the dipoles (b).*

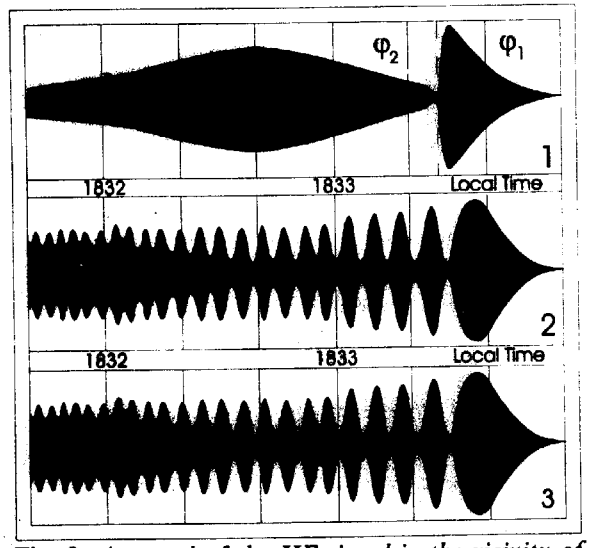

Fig. 2. *A record of the HF signal in the vicinity of the SCT (channel 1 - the "North-South" arrey of the UTR-2; channels 2 and 3 - crossed dipoles of a polarimeter).*

motion and also to find the velocity V and motion direction γ of the signal diffractive pattern along the Earth's surface:

$$\gamma = \arctan\{1 - 2\Delta t_{2-3}/\Delta t_{2-1}\},$$
$$V = 2l\cos\gamma/\Delta t_{2-1}, \qquad (1)$$

where l is the spatial separation of the dipoles; Δt_{i-j} is the time lag between the moments of appearance the same interference minimum at the antennas i and j. As is known [Bremmer, 1949], the field structure like presented in Fig.1a is caused by superposition of two rays: the lower and the upper (Pedersen) one. This fact is especially evident in Fig.2 showing the data obtained with the use of crossed antennas of a polarimeter (channels 2 and 3) and the North-South array of the UTR-2 (channel 1) characterized by a high directivity in the elevation angle plane. The synchronous fadings in the two polarimeter channels are evidence for the interference of two waves of the same polarization, i.e. the lower and upper rays. At the same time, there are no interference fadings in the channel of the directional antenna. The smooth variation of the signal envelope here reflects variations of the elevation angle of the ray separated by the antenna, while orientation of its reception pattern has remained fixed (the reorientation moment is shown with the dashed line in Fig.2). It indicates that the reception pattern of the North-South array is narrow enough to separate a single ray (in this case it was the lower ray). Analysis of the interference structure of the signal shows that the shorter is the distance between the CST and a receiver, the greater beat periods and fading depth of the signal amplitude. This implies bringing the lower and upper ray trajectories together until they become physically undistinguishable. Knowledge of the shape of the antenna pattern and its orientation allows measuring time dependences of the elevation angles of the lower and upper rays ($\varepsilon_l(t)$ and $\varepsilon_u(t)$, respectively). Along with this, there is no problem in measuring the phase difference $\Delta\Psi_{l-u}(t)$ between the spatial components and amplitudes of the interfering waves, $a_l(t)$ and $a_u(t)$. In addition to the

analysis of the signal envelope it is possible to register the Doppler spectra of the signals. In Fig.3 the spectra of the signals presented in Fig.2 are shown. The integration time T with which the spectra were obtained was 10s, the spectral line resolution is 0,1 Hz. The origin of the vertical coordinate corresponds to the carrier frequency f_0 of the transmitted signal. As the distance between the CST and the receiver becomes shorter, the phase paths of the rays lengthen and Doppler frequency shifts of the upper and lower rays ($F_{Dl}(t)$ and $F_{Du}(t)$ respectively) have negative sign. In the nearest vicinity of the caustic the rays prove to be undistinguishable in the frequency domain as well. The above described results correspond to focusing of the extraordinary "X"-wave that occurs on a single-hop radio path near the sunset time (the CST moves toward the transmitter). Actually after "X"-wave focusing one can see focusing of the ordinary component "O" of the probing signal. When the CST moves from the transmitter (usually it being near the sunrise), the inverse development of the events is observed. Usually by the moment of focusing of the "O"-wave the upper ray of "X"\ polarization has been damped and there remain three significant components in the resulting signal: lower rays of the "O" and "X" polarizations and upper ray of the "O" polarization. Generally, the "O" and "X" components can be reliably separated in the frequency domain, while the spatial filtering does not allow resolving them because their trajectories are too close to each other.

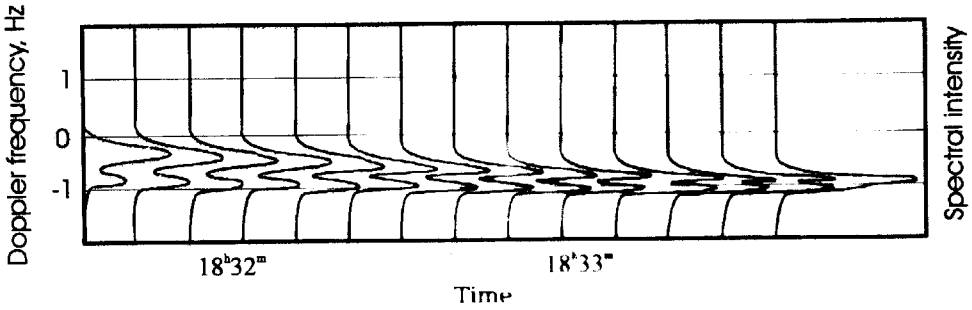

Fig. 3. *Time sequences of the spectra of the signal plotted in the Fig. 2. (channel 2).*

Analysis of the time dependences $\Delta\Psi_{l,u}(t)$, $a_l(t)$ and $a_u(t)$ shows that they are not always monotonic functions. As a rule, there are some random fluctuations in these parameters caused by ionospheric irregularities. These variations are especially strong when the spatial scale-size of the irregularities l is commensurable with the first Fresnel zone $\sqrt{\lambda D}$ (λ being the wavelength of the propagating signal and D the path length). If such disturbances are powerful enough, then the "shadow-light" boundary spreads out and the interference structure of the signal becomes more complicated. Several years of investigations of this effect have shown that for midlatitude single-hop radio paths the Fresnel-size irregularities have a strong effect on the near-caustic fields in about 30 % of the day-time measurements and 40 % to 50 % at night. Comparison of the results with the data of vertical ionospheric sounding data obtained in the vicinity of the radio path can allow concluding that the events coincidence in time with F-scattering.

4. Formulating and solving the problem of ionospheric sounding

The motion of the CST relative an observer due to the regular and stochastic variations of the electron density profile, as has been mentioned, leads to extremely strong changes in the parameters of the resulting field. It is worth noting, that when the CST passes across the reception site, the signal strength changes by tens of dB over distances of a few hundred meters, while far off the caustic its typical attenuation is units of dB per 1000 km [Davies, 1990]. Since the integral representation of the near-caustic fields providing an uniform asymptotic expansion is rather complex, any attempts of solving the inverse problem in the nearest vicinity of the caustic face difficulties of principle that have not been overcome until now. At the same time, in the illuminated zone near the SCT, beginning from the first interference minimum, the ray-optical approximation is accurate enough to be used. Special investigations of this problem using the interference integral technique [Anyutin, et al., 1985] have shown, that within the measurement accuracy, the inadequacy of the ray-

optical approximation is not essential. These results allow using the ray-optical approximation for solving the inverse problem of ionospheric sounding.

To demonstrate the possibility of solving the problem of ionospheric diagnostics with the use of the near-caustic field measurements, let us consider the simplest ionospheric model, namely the parabolic electron density profile. For a plane-stratified isotropic ionosphere the electron density profile can be written as

$$N_e(z) = \begin{cases} N_m\left[1-(z_m-z)^2/y_m^2\right], \\ 0, \end{cases}$$
$$z \in |z_m - z| \qquad (2)$$
$$z \notin |z_m - z|$$

Here N_m and z_m are the magnitude and location of the electron density maximum, respectively and y_m is the half-thickness of the ionospheric layer. As is known [Davies, 1990], the dependence of the horizontal distance D on the elevation angle ε is determined, in the case of single-hop propagation and the profile of equation (2), by the relation:

$$D = 2z_0 \cot\varepsilon + y_m \alpha \cos\varepsilon \ln\frac{1+\alpha\sin\varepsilon}{1-\alpha\sin\varepsilon}, \quad (3)$$

where $\alpha = f/f_{cr}$; f_{cr} is the critical frequency (i.e. the highest plasma frequency) of the ionosphere. It is easy to derive the expression for the eikonal

$$\Psi = \frac{2z_0}{\sin\varepsilon} + y_m \sin\varepsilon + \qquad (4)$$
$$+\frac{y_m}{2}\left[\alpha + \alpha\cos^2\varepsilon - \alpha^{-1}\right]\ln\frac{1+\sin\varepsilon}{1-\sin\varepsilon}$$

Using equations (3) and (4), it is possible to derive a set of equations like

$$\begin{cases} \varepsilon_l\left[z_0(t_i), y_m(t_i), f_{cr}(t_i)\right] = \varepsilon_l(t_i), \\ \varepsilon_u\left[z_0(t_i), y_m(t_i), f_{cr}(t_i)\right] = \varepsilon_u(t_i), \\ \Delta\Psi_{l-u}\left[z_0(t_i), y_m(t_i), f_{cr}(t_i)\right] = \Delta\Psi_{l-u}(t_i). \end{cases} \qquad (5)$$

The equation set (5) is complete, which allows determining the unknown parameters of the model $z_0(t_i)$, $y_m(t_i)$ and $f_{cr}(t_i)$ for the time moment t_i, using the measured values $\varepsilon_l(t_i)$, $\varepsilon_u(t_i)$ and $\Delta\Psi_{l-u}(t_i)$. The set can be solved numerically [Bliokh et al., 1986], as illustrated in Fig.4. These are constant-value curves for the lower ray elevation angle ε_l and phase path difference $\Delta\Psi_{l-u}$. The curves have been drawn for a fixed half-thickness y_m (its value can be determined, for example, from other independent data) and path length D as functions of the ionospheric boundary height z_0 and ratio of the operating frequency f_0 to the critical one f_{cr}. Obviously, knowledge of the values ε_l and $\Delta\Psi_{l-u}$ at the time moments t_i allows determining unambiguously the ionospheric parameters z_0 and f_{cr} for the same moments, as coordinates of the intersection points of the appropriate curves ($\Delta\Psi_{l-u} = const$ and $\varepsilon_l = const$). An example of recovering $z_0(t)$, $y_m(t)$ and $f_{cr}(t)$ in this technique for two cases - near the sunrise and sunset, is shown in Fig.5.

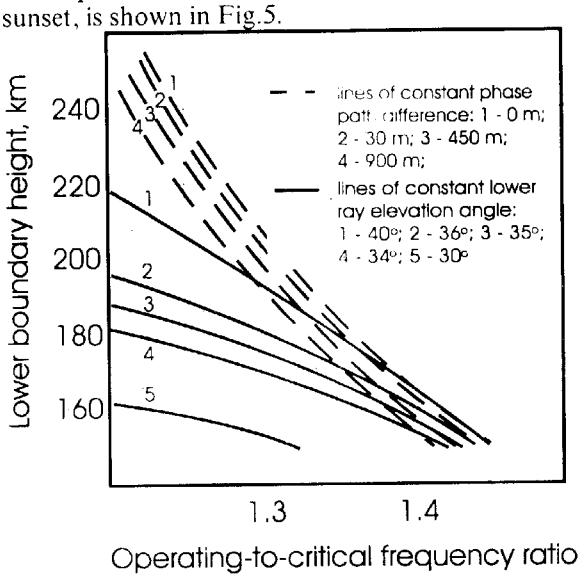

Fig. 4. *Constant-value lines of the phase path difference between the lower and the upper ray, and elevation angle of the lower ray for fixed half-thickness.*

Of principal importance for the restoration technique are the uniqueness and correctness of the inverse problem. These have been checked in three types of tests. The first one was based on comparison of the restored parameters with the data obtained simultaneously in a different technique, for example, vertical ionospheric sounding. The gist of tests of the second type consists in the analysis of the excess data measured and calculated for the determined ionospheric parameters that have not been used for the restoration, for example, Doppler frequency shifts for the lower, F_{Dl}, and upper, F_{Du}, rays. While conducting the third type of the tests, multifrequency measurements were used. All the above mentioned signal parameters were measured for each of the frequencies. Then, using the data obtained for one of these

frequencies, parameters of the ionospheric layer were restored. These were used to calculate signal parameters at other frequencies for ultimate comparison with the measurements. The agreement was assumed as satisfactory if the data differed from each other by a smaller value than the measuring accuracy, that is $\Delta\varepsilon \le 0{,}5^{\circ}$ and $\Delta F_D \le 0{,}05\ Hz$. All the tests have demonstrated the high accuracy of the procedure suggested for restoration of the ionospheric parameters.

A further refinement of the ionospheric model, namely employment of a biparabolic plasma layer (layers E and D), has not furnished a significant correction to the restored electron density profile near its main maximum if $F_{MUFF} > F_{MUFE}$. That is only natural as the major general contribution to the near-caustic fields is given by the rays reflected in the vicinity of the main ionospheric maximum where the parabolic approximation is suitable. In the lower ionosphere the lower and upper ray trajectories are practically indistinguishable so that the near-caustic field parameters depend but weakly on the electron density profile in this range.

Taking the geomagnetic field into account (i.e. using both the "O" and "X" focusing) has not revealed a significant influence upon the results of solving the inverse problem. However, it has allowed determining the magnitude of the electron gyrofrequency.

It is clear that for the plane-stratified ionosphere the "shadow-light" boundary looks like a circle around the transmitter. Hence, the SCT always moves exactly towards or from the transmitter because the normal to the SCT is oriented along this direction. In the presence of horizontal gradients of the electron density the shape of the "shadow-light" boundary becomes more complicated, which, in its turn, leads to a deviation of the motion direction from the transmitter azimuth. The effect is particularly bright in the vicinity of the sunrise/sunset or when the TIDs pass through the reflecting region. An example of the data obtained at dusk for a set of experiments using the triangulation technique is shown in Fig.6. The measured data are represented in polar coordinates showing the velocities (radii) and directions (angles) of the SCT motion, the dashed line is oriented toward the transmitter. One can see that the points lie mostly on the right side of the dashed line. This corresponds completely to the gradients that most likely occur near the sunset. Comparison of these data with calculations in a model with a slant ionospheric layer has allowed evaluating the angle characterizing horizontal gradients in the ionosphere [Galushko, 1984]. In our measurements, its average value was about -5° and maximum approached -10° to -12° for near-sunset time when most experiments of this kind were conducted.

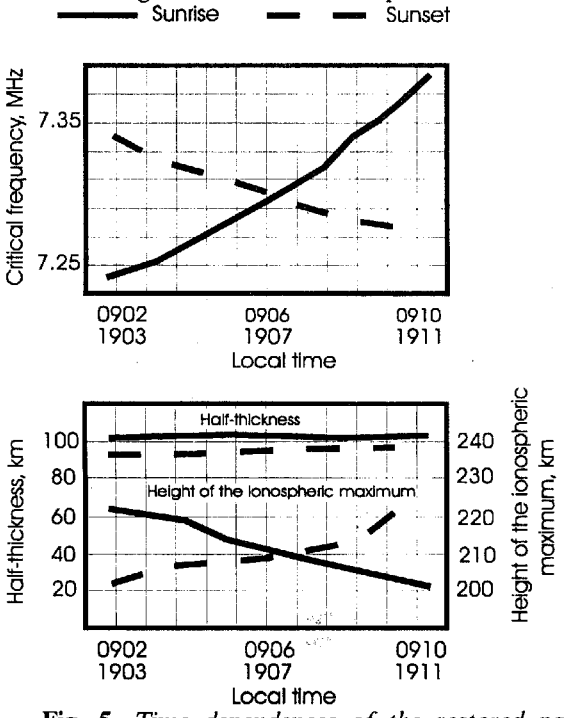

Fig. 5. *Time dependences of the restored parameters of the model ionospheric layer the sunrise and sunset.*

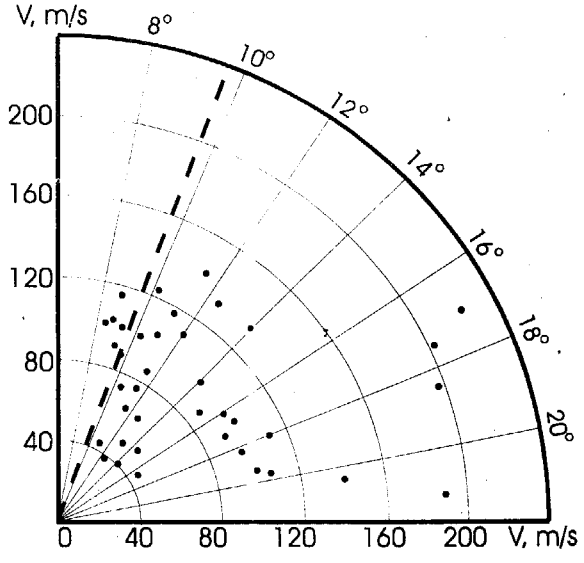

Fig. 6. *Velocity and motion direction of the precaustic field pattern near sunset.*

So far we have analyzed the HF trajectory parameters only. Now let us consider the behaviour of the HF signal envelope in the vicinity of the SCT. For this purpose we have analyzed dependences of a parameter m versus the distance D. The value m is determined for a set of discrete points D_i as

$$m(D_i) = \frac{A_{\max}(D_{i+1}) - A_{\min}(D_i)}{A_{\max}(D_{i+1}) + A_{\min}(D_i)}, \qquad (6)$$

where $A_{\max}(D_{i+1})$ and $A_{\min}(D_i)$ are the maximum and the minimum value of the signal envelope, respectively, for corresponding distances; recalculation of the time dependences into range has been made on the assumption of uniform motion. Analysis of the data has shown that in a number of cases the parameter $m(D_i)$ decreases at longer range D faster than it follows from the calculations made for the restored ionospheric parameters. The effect apparently being due to propagation losses, we have introduced the effective collision frequency ν_e of electrons, such that the refractive index $n(z)$ of the ionosphere takes the form

$$n^2(z) = 1 - \frac{\varpi_{cr}^2(z)}{\varpi_0(\varpi_0 - i\nu_e)}\left[1 - \left(\frac{z - z_m}{y_m}\right)^2\right] . \qquad (7)$$

The value ν_e has been assumed independent of height z, which is quite realistic for the ionospheric F layer [Alpert,1972]. Absorption in the lower ionosphere (E and D layers) was also neglected because the difference between the upper and lower ray trajectories depended primarily on the F layer parameters. As follows from numerical estimates, the contribution of the lower ionosphere absorption into m is about ten times smaller than that of region F. The calculations were made in the interference integral technique [Anyutin, et al., 1985] and some results are shown in Fig.7. It represents range dependences of the signal envelope A (relative units) calculated for a set of values $s = \nu_e/\varpi_0$. As can be seen, the envelope maxima and minima practically are not displaced as s increases. The magnitude of the maxima decreases significantly, while the minimal amplitude changes only slightly. Fig.8 shows range dependences of the parameter m for a set of values of ν_e (solid lines), and measured results for two observational days(crosses and points, respectively). Comparison of the measured data with the calculations allows determining the effective collision frequency ν_e of electrons (this case equal to $\sim 1{,}2 \times 10^3 s^{-1}$ for one day and $\sim 3{,}1 \times 10^3 s^{-1}$ for the other). To test correctness of the method for measuring the effective electron collision frequency, the following experiments were conducted. On a midlatitude radio path about 940 km in length the value ν_e was determined simultaneously in the above described technique and by means of the A1 method with the use of a vertical ionospheric sounder located in the vicinity of the middle point of the radio path [Beley, et al., 1990]. Comparison of the data demonstrated their good mutual agreement. The apparent overestimation of ν_e is a result of the signal scattering by the medium-scale ionospheric irregularities which produced additional attenuation of the coherent component of the probing signal.

Along with the additional attenuation of the near-caustic signals, ionospheric irregularities produce distortions of the field pattern, bringing forth, for example, variations of the positions of the resulting field minima. These manifest themselves, in particular, through non-monotonic dependences of the periods of the interference fadings versus time. In its turn, the ionospheric disturbances bring in some additional errors in the ionospheric parameters restored.

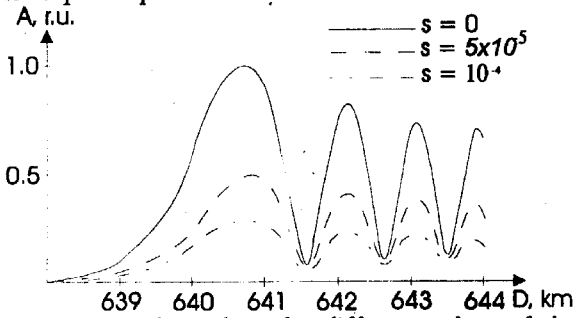

Fig. 7. *Signal envelope for different values of the parameter* $s = \nu_e / \varpi_0$

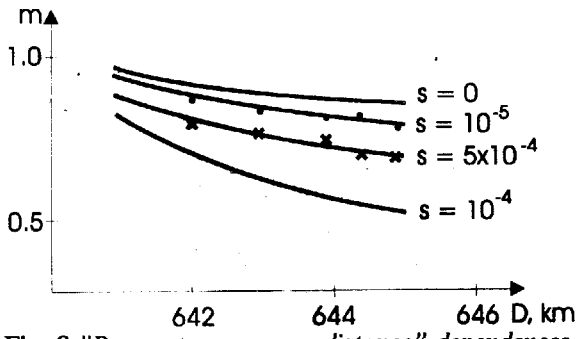

Fig. 8. *"Parameter m versus distance" dependences, calculation (curves) and measurement on two observation days*

Investigations of the influence of ionospheric irregularities upon the near-caustic field pattern

were conducted in the ray optical approximation using the perturbation method for eikonal. Medium-scale irregularities ($L \cong 10...50\ km$) alone were taken into account. This is stipulated, on the one hand, by the high degree of spatial correlation of the near-caustic fields for the distances $d \cong 2km$, which allowed neglecting irregularities of scale-size $L < d$. On the other hand, the large scale-size disturbances with $L \geq y_m$ do not produce significant variations of the fading periods of the resulting field. As a result, it has been shown that the ionospheric irregularities cause shifting, on the average, positions of the interference minima towards the SCT on the value

$$\Delta x_j = x_{0j} - < x_j > = \frac{S_j^2}{2} \times$$

$$\times \frac{\left(\partial D/\partial\varepsilon\right)^{-1} \sin\varepsilon\Big|_{\varepsilon=\varepsilon_{lj}} - \left(\partial D/\partial\varepsilon\right)^{-1} \sin\varepsilon\Big|_{\varepsilon=\varepsilon_{uj}}}{\left(\cos\varepsilon_{lj} - \cos\varepsilon_{uj}\right)^3}, \quad (8)$$

where x_{0j} is the undisturbed position of the j-th minimum; S_j^2 is determined as

$$S_j^2 = < \delta\Psi_l^2\left(x_{0j}\right) > + < \delta\Psi_u^2\left(x_{0j}\right) > -$$

$$- 2 < \delta\Psi_l\left(x_{0j}\right)\delta\Psi_u\left(x_{0j}\right) >;$$

$\delta\Psi_l$, and $\delta\Psi_u$ are fluctuations of the eikonal for the lower and the upper ray respectively; and the angular brackets denote averaging. Also estimated were the errors of the ionospheric critical frequency and variance of the periods of the signal fading. Comparing these data with the measurements makes it possible to estimate the most probable values of the parameters of ionospheric disturbances, namely the characteristic size has been found to equal $L \cong 15km$ and intensity of the fluctuations $< (\delta N)^2 >^{1/2} / N_m$ lies within the interval $10^{-2}...10^{-3}$.

It is clear that wider employment of the proposed methods of ionospheric diagnostics is restricted by the necessity of using highly directional antennas capable of resolving the interfering signals in elevation angle. Meanwhile, the diagnostics has been extended to allow near-caustic field measurements with a set of spaced small-size antennas (single dipoles) [Anyutin, et al., 1990]. The gist of the method is as follows. For the parabolic model of the ionosphere, the set of equations can be derived using (3) and (4), (9).

$$\begin{cases} \Psi_l - \Psi_u = F_1\left(\varepsilon_l, \varepsilon_u, z_0, y_m f_{cr}\right) = \Delta\Psi_{l-u}, \\ D - 2z_0 \cot\varepsilon_l - y_m \alpha \cos\varepsilon_l \ln\dfrac{1+\alpha\sin\varepsilon_l}{1-\alpha\sin\varepsilon_l} = F_2\left(\varepsilon_l, z_0, y_m, f_{cr}\right), \\ D - 2z_0 \cot\varepsilon_u - y_m \alpha \cos\varepsilon_u \ln\dfrac{1+\alpha\sin\varepsilon_u}{1-\alpha\sin\alpha_u} = F_2\left(\varepsilon_u, z_0, y_m, f_{cr}\right). \end{cases}$$

Table 1.

Results of the ionospheric parameter restoration

$f_0\ Mhz$	Ionospheric parameters	Spaced Dipoles	UTR-2
10	f_{cr}, MHz	7.15	7.2
	z_0, km	141.9	150
	y_m, km	95.5	100
	$\theta_{0,deg}$	40.3	39.7
12	f_{cr}, MHz	8.81	8.8
	z_0, km	140	150
	y_m, km	97.5	100
	$\theta_{0,deg}$	40.3	40.3

The set has been written for some fixed distance D and involves 5 unknown parameters, namely, z_0, y_m, f_{cr}, ε_l and ε_u. If the measurements of $\Delta\Psi_{l-u}$ were performed at least at three spaced points, then a set of 9 equations can be derived for 9 unknown values: $z_0, y_m, f_{cr}, \varepsilon_{l1}, \varepsilon_{u1}, \varepsilon_{l2}, \varepsilon_{u2}, \varepsilon_{l3}$, and ε_{u3}. Solution of the system can be found numerically in the Ψ-conversion technique[Chichinadze, 1983]. The results of restoring ionospheric parameters in this approach and those obtained simultaneously through angular measurements with the UTR-2 are shown in Table 1.Comparison of the data shows that they are in good agreement. This allows practical application of ionospheric diagnostics not only with the unique antenna array like UTR-2, but with single spaced dipoles, too

5. Conclusion

Measurements of the diffractional HF field pattern in the vicinity of the skip distance and further comparison with theory allow recovering a number of ionospheric parameters, such as the model electron density profile, effective collision frequency of the electrons, horizontal gradients of the electron density and parameters of medium scale ionospheric disturbances. Comparison of these data with the results obtained simultaneously in another technique of ionospheric diagnostics (for example, vertical sounding) has shown a high accuracy of the methods proposed for iono-

spheric sounding. In particular, the regions of natural field localization near the caustic have proven very suitable for ionospheric diagnostics. E.g., the accuracy of the developed method for determining the layer height and the critical frequency is 5 km and a few KHz, respectively, which is comparable with the potentialities of modern vertical and oblique ionospheric sounders. A great advantage of the methods described is their ecological harmlessness, in the sense that they require no dedicated transmitters but employ the already existing broadcasting stations as sources of the probing signals. The great number of such stations and the relative simplicity of the proposed techniques permit expecting a wide practical employment of the developed methods.

Acknowledgment

The authors deem it their pleasant duty to acknowledge the contribution of their teacher Prof. P.V.Bliokh into these investigations that were started on his initiative. We are also thankful to Dr. A.P.Anyutin and Prof. P.F.Denisenko who co-authored a number of papers on the subject, and to Dr. V.S.Beley who participated in developing the receiving complex and conducting the numerous measurements.

The research described in this publication was made possible in part by Grant # U-36000 from the International Science Foundation.

References

1. Alpert Ya.L. Electromagnetic Wave Propagation and the Ionosphere. Moscow. Nauka, 1972.

2. Anyutin A. P. and Borovikov V.A. Preprint, IRE AN USSR. Moscow, 1984. № 42.

3. Anyutin A. P., Galushko V.G., and Yampolski Yu.M. Izvestiya vysshikh uchebnykh zavedenii, seriya Radiofizika, 1985, 28, 247.

4. Anyutin A. P., et al. Geomag. Aeron., 1990,30, 156.

5. Argo P. E., Reliability Calculations and Above-the-MUF Propagation, Proceedings and Program for the 7th Int. Ionospheric Effects Symp., Alexandria, VA, May 1993.

6. Babitch V. M., Molotkov I.A., and Popov M.M. Preprint IRE AN USSR. Moscow, 1984, № 24.

7. Beley V. S., et al. Geomag. Aeron., 1990, 30, 979.

8. Bliokh P. V., Galushko V.G., and Yampolski Y.M. In: Problems of diffraction and wave propagation, Univ. of Leningrad, Issue 20, 1986, 153-165.

9. Braude S.Ya., et al. Astrophysics and Space Science, 1978. 54, 3.

10. Bremmer H. Terrestrial Radio Waves, Amsterdam, Elseiver Publ. Co., 1949.

11. Chernov Yu. A. and Zhyltsov A.U. Geomag. Aeron., 1982, 22, 508.

12. Chichinadze, V.K., Analysis of non-convex non-linear optimization problems. Moscow. Nauka, 1983.

13. Davies K. Ionospheric Radio Waves. London. Peter Peregrinus Ltd., 1990.

14. Galushko V. G. Izvestiya vysshikh uchebnykh zavedenii, seriya Radiofizika, 1984,27, 1491.

15. Kryukovski A. S., Lukin D.S., and E.A.Palkin. Preprint. IRE AN USSR. Moscow, 1984. № 41.

16. Taraschuk Yu. E., et al. Geomag. Aeron., 1982, 22, 505.

17. Warren R. E., De Witt R.N., and Warber C.R. Radio Sci., 1982,17. 514.

Прикаустические поля и ионосферная диагностика

В.Г.Галушко, Ю.М.Ямпольский

Описаны результаты исследований пространственно-временной структуры КВ полей в окрестности мертвой зоны. Данные получены на среднеширотной радиолинии длиной менее 1000 км с использованием широковещательных станций в качестве источников пробных сигналов. Отраженные от ионосферы сигналы принимались и обрабатывались с помощью многоканального когерентного приемника и крупнейшей исследовательской фазированной антенной решетки декаметрового радиотелескопа УТР-2. Сильная зависимость параметров зондирующих волн от состояния ионосферной плазмы позволила сформулировать и решить ряд модельных обратных задач ионосферной диагностики. Это дает возможность определять параметры параболического ионосферного слоя, эффективную частоту соударений электронов, оценить величину горизонтальных градиентов электронной концентрации и некоторые параметры среднемасштабных ионосферных неоднородностей. Ряд проверок, выполненных как в рамках предложенного метода, так и путем сопоставления восстановленных параметров с данными других диагностических средств, свидетельствуют о высокой эффективности и точности описанного в статье подхода.

Прикаустичні поля та іоносферна діагностика

В.Г. Галушко, Ю.М. Ямпольский

Описано результати досліджень просторово-часової структури КХ полів поблизу

мертвої зони. Дані були отримані на середньоширотній радіотрасі довжиною меньше 1000 км з використанням широкомовних станцій як джерел пробних сигналів. Відбиті від іоносфери сигнали приймалися та оброблялися за допомогою багатоканального когерентного приймача та найбільшої дослідницької фазованої антенної решітки декаметрового радіотелескопу УТР-2. Різька залежність параметрів зондуючих хвиль від стану іоносферної плазми дозволила сформулювати та вирішити ряд модельних зворотних задач іоносферної діагностики. Цедіє можливість визначити параметри параболічного іоносферного шару, ефективну частоту зіткнення електронів, оцінити величину горизонтальних градвєтнтів електронної густини та деякі параметри параболічного іоносферного шару, ефективну частоту зіткнення електронів, оцінити величину горизонтальних градієнтів електронної густини та деякі параметри середньомасштабних іоносферних неоднорідностей. Ряд перевірок, що були виконані як у рамках запропонованого методу, так і шляхомпорівняння відтворених параметрів з даними інщих діагностичних засобів, свідчать про високу ефективність та точність описаного у статті підходу.